JOURNAL OF CATALYSIS 134, 226–241 (1992)

Direct Synthesis of Methanol, Dimethyl Ether, and Paraffins from Syngas over Pd/Zeolite Y Catalysts

F. A. P. CAVALCANTI, A. YU. STAKHEEV, AND W. M. H. SACHTLER

V. N. Ipatieff Laboratory, Center for Catalysis and Surface Science, Northwestern University, Evanston, Illinois 60208-3000

Received June 28, 1991; revised September 20, 1991

CO hydrogenation has been studied over Pd/NaY and Pd/HY catalysts prepared by ion exchange. By controlling the calcination program, Pd/NaY catalysts can be tuned to selectively produce either branched C_{4+} hydrocarbons or CH_3OH and CH_3OCH_3. On Pd/HY catalysts, C_2H_6 and C_3H_8 predominate. Dissociative adsorption of CO over small Pd particles leads to formation of methane and an interstitial $PdC_{0.13}$ compound, detected by XRD. Reduction with H_2 converts $PdC_{0.13}$ to Pd and methane. During CO hydrogenation catalysis, palladium particles grow, leading to local collapse of the zeolite lattice. Pd migration is also manifest from changes in the Pd/Si ratio detected by XPS. The reaction network reveals bifunctional catalysis: formation of CH_3OH on Pd particles is followed by its conversion to CH_3OCH_3 and hydrocarbons over acid sites. Readsorption of hydrocarbons on the Pd particles results in hydrogenation of unsaturated compounds and to changes in the activity, selectivity, and deactivation behavior of the catalysts.

INTRODUCTION

The chain-growth mechanism of the Fischer–Tropsch Synthesis (FTS) imposes serious restrictions on the selective conversion of syngas to high octane fuels and other chemicals. There have been several attempts to find alternative paths for CO hydrogenation. In the late 1940's and early 1950's, Pichler (*1*) reported the selective conversion of syngas to branched hydrocarbons, mainly C_4's and C_5's, over thorium oxide and other basic oxide catalysts. A drawback of this "iso-synthesis" is that it requires very high reaction temperature and pressure (450°C and 300–600 atm). A much more successful approach was pioneered by Mobil. In this process syngas is first converted to methanol, which is then reacted, in the methanol-to-gasoline (MTG) process, over the acid form of the zeolite ZSM-5 to form high octane gasoline (*2*). Only the high aromatic content of the product is causing some concern in view of its effect on the environment.

Palladium has been known since 1978 to be an active catalyst for syngas conversion to methanol (*3*). The mechanism of this reaction is, however, still controversial. Although CH_3OH synthesis has been reported on Pd single crystals (*4*), other authors claim that evidence for this reaction to take place on unpromoted Pd is inconclusive; it is proposed that $Pd^{\delta+}$ sites created by intentionally or unintentionally added promoters are essential for this reaction (*5*). Other controversial points include the question whether nondissociative CO adsorption on Pd is accompanied by some dissociative adsorption and the structure sensitivity of CH_3OH synthesis on this catalyst.

Attempts have been made to couple the synthesis of methanol with its conversion to other products, in order to overcome the thermodynamic limitations of the syngas/methanol equilibrium. These include the use of physical mixtures of ZSM-5 with an iron catalyst (*6*), ZrO_2, or Zn/Cr (*7*); likewise, mixtures of Pd/SiO_2 with HY, H-mordenite, and HZSM-5 (*8*) have been tested. Bifunctional catalysts were prepared by impregnation of Pd on zeolites Y (*9, 10*), ZSM-5

0021-9517/92 $3.00

(*9, 11*), and the molecular sieve SAPO (*12*), and by ion exchange of Pd into Y (*13, 14*) and X (*15*) zeolites. Many of these studies revealed encouraging results, but no systematic study of the underlying concept has been published.

The objective of the present study is to address the use of ion-exchanged Pd/Y catalysts for syngas conversion to CH_3OH/CH_3OCH_3 and/or hydrocarbons. This work is largely motivated by recent progress in unraveling the atomic processes in the genesis and growth of Pd particles inside NaY (*16*) and the fairly detailed understanding of some of the intriguing interactions that take place between CO molecules and zeolite-encaged Pd particles (*17–22*). The main emphasis of the present study is, therefore, laid on the remarkably dynamic nature of the chemical and physical processes inside the Pd/Y catalyst during CO hydrogenation.

EXPERIMENTAL

Catalyst Preparation

Catalysts were obtained by ion exchange of NaY (Linde LZY-52) or HY (prepared by the calcination of NH_4Y, Linde LZY-82, at 500°C for 2 h in pure O_2) with a dilute aqueous solution of $[Pd(NH_3)_4](NO_3)_2$ (Johnson Matthey Electronics or Alfa Chemicals) to obtain a nominal 4 wt% Pd loading. Details of the preparation procedure have been given elsewhere (*16*). Analysis of the catalysts showed that for Pd/NaY and Pd/HY the actual Pd (determined by ICP) and Na (determined by AA) contents were 3.45 and 5.26 wt%, and 2.50 and less than 0.15 wt%, respectively.

Reaction Studies

CO hydrogenation at various temperatures and 10–11 atm total pressure was carried out in a continuous-flow fixed-bed reactor system (Max II Unit, Xytel Corp.). A CO/H_2 mixture (Linde, UHP, $CO:H_2$ = 1 : 1) was used and further purified by alumina and activated charcoal traps. The catalysts were calcined *ex situ* by heating (0.5°C/min) in pure O_2 (Linde, UHP) to the desired temperature, T_c (2 h). The catalysts were then stored until they were loaded in the reactor for reduction. Reduction was carried out by heating (about 1°C/min) 0.8 g of the catalyst *in situ* in flowing He (Linde, UHP) to the desired temperature, T_r, and then changing to a stream of pure H_2 (Linde, UHP) for 1 h. After reduction the catalyst was brought to the reaction temperature in a stream of He over a period of at least 30 min. Hereafter, the pretreatment conditions of each catalyst will be designated by Pd/Y(T_c/T_r). Product analysis was carried out on-line using a Hewlett–Packard 5890 GC fitted with a 50-m PONA capillary column and FID. The transfer line from the reaction system to the GC consisted of 3.18-mm (0.3 mm)-o.d. Teflon PFA tubing heated to 125°C.

XRD and XPS Characterization

Powder X-ray diffraction was carried out using Ni-filtered Cu$K\alpha$ radiation at 50 kV and 25 mA with a Rigaku Geigerflex diffractometer. Continuous scans in the 2Θ region from 10 to 50° with a 0.02° step were recorded. All samples were studied *ex situ* in air and were not rereduced (except where noted) prior to analysis. XPS results were obtained using a VG ESCALAB-5 spectrometer using unmonochromatized Al$K\alpha$ radiation. The samples were rereduced *in situ* at 150°C before measurement. The binding energy of the Si 2*p* line was used as an internal standard. Values of the modified Auger parameter for Pd were also determined by monitoring the X-ray excited M_5VV transition (*23*).

RESULTS

Reaction Studies

Pd/NaY. Figure 1 shows typical time-on-stream behavior for two Pd/NaY catalysts, Pd/NaY(500/350) (Fig. 1A) and Pd/NaY(250/250) (Fig. 1B). In this figure, the rate of carbon output in each product fraction has been normalized by the rate of carbon output in CH_4 at 15 min reaction (first reaction sample). It is clear that in both

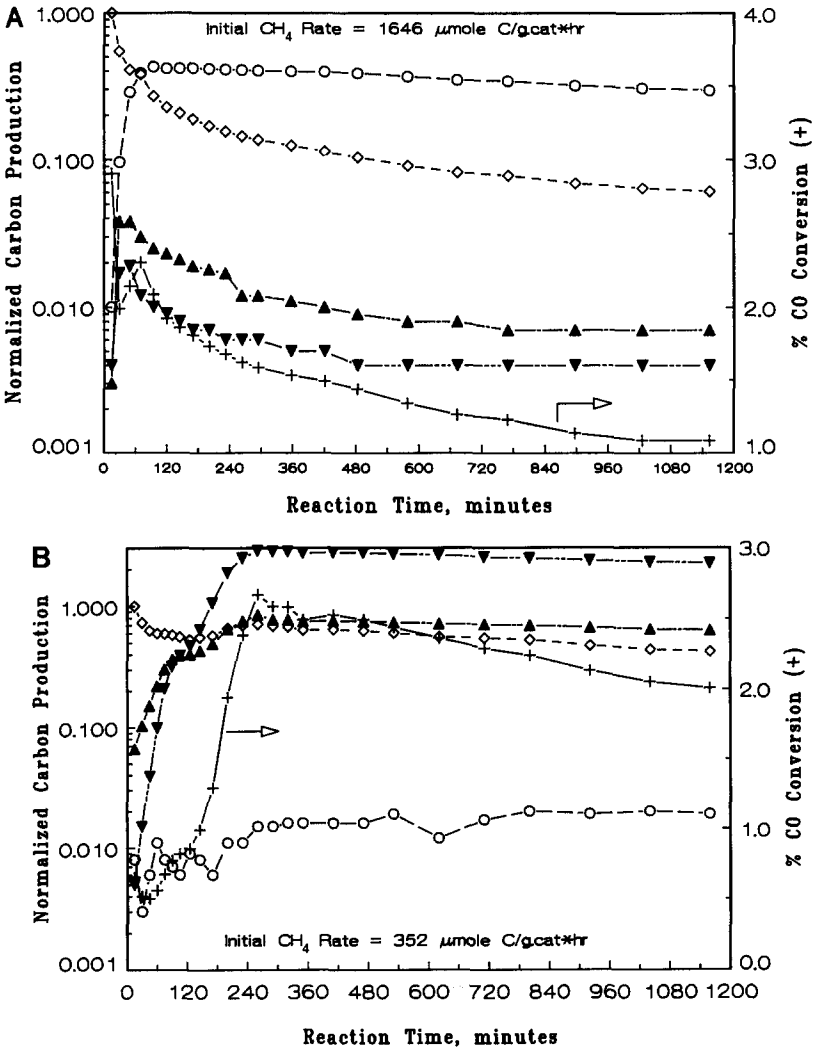

FIGURE 1

cases drastic changes in the rates of product formation take place in the first few hours of reaction. CH_4 is the predominant product at the start of the reaction on these catalysts. However, its rate of formation drops off rapidly and after 2 h on-stream it has been reduced to at least half of its initial value. In contrast, during this same period the formation of other products rises significantly.

In the case of Pd/NaY(500/350), Fig. 1A, the rates of CH_3OH and CH_3OCH_3 formation increase sharply and reach a maximum by the end of the first hour of reaction. Higher hydrocarbons (two carbon atoms or more) production also rises markedly during this period, and about 2 h into the reaction these products as a class become the predominant pathway for carbon output in the reaction. For the remainder of the reaction there is little deactivation in higher hydrocarbons production while rates of CH_4, CH_3OH, and CH_3OCH_3 formation decrease steadily.

In the case of Pd/NaY(250/250), Fig. 1B, there are increases of at least one order of magnitude in the rates of CH_3OH and

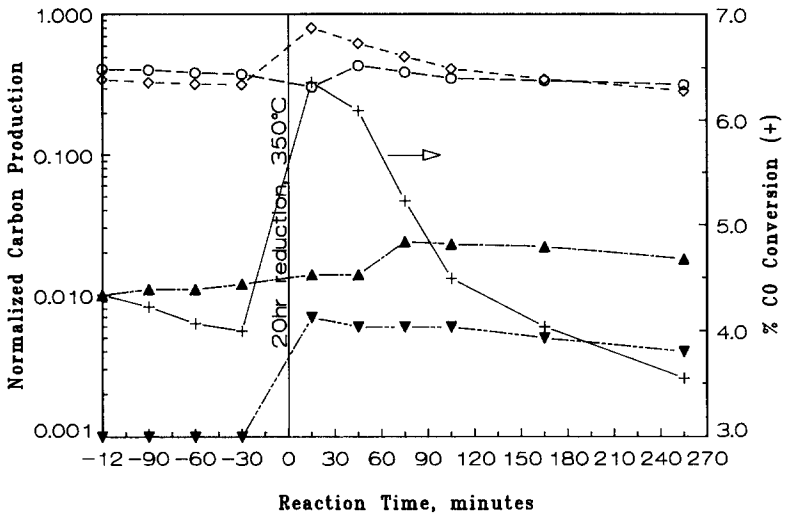

FIGURE 2

CH_3OCH_3 formation during the first 2 h of reaction. After this period there is little deactivation in the formation of these two products while CH_4 production decreases steadily. Formation of higher hydrocarbons is not significant with this catalyst, accounting for less than 4% of carbon in the products.

The effect of H_2 reduction on the deactivated catalyst is shown in Fig. 2. A fresh batch of Pd/NaY(500/350) was reacted at 285 ± 2°C, 11.0 ± 0.3 atm and GHSV = 1800 ± 100 h^{-1} for 20 h. The space velocity was then lowered to 900 ± 50 h^{-1} for 2 h and then to 400 ± 25 for another 2 h. After this reaction period the catalyst was reduced in 8 atm of pure H_2 at 350°C for 20 h. During this reduction period CH_4 was detected in significant amounts, in particular during the first few hours of reduction. The temperature was then lowered under He flow to the previous reaction temperature and a new reaction period at GHSV = 400 ± 25 h^{-1} was started. As can be seen from Fig. 2, this reduction resulted in an increase in CO conversion by, initially, some 60%. Most of this increase can be attributed to more than doubling of the rate of CH_4 production; it subsequently decreases rapidly returning to the value at the end of the first reaction period. It is interesting to note that the long reduction period does not significantly affect the rate of CH_3OH and higher hydrocarbons formation.

The higher hydrocarbons carbon selectivity for Pd/NaY(500/350) is shown in Fig. 3 along with the selectivity to branched paraffins. The latter constitute at least 70% of each product fraction. The C_{7+} carbon fraction includes hydrocarbons up to C_{10} but no aromatic products (benzene, toluene, xylenes = BTX) were detected. Olefins account for less than 3% of each carbon fraction. Clearly, this catalyst is very selective for the formation of higher hydrocarbons with four or more carbon atoms.

The effect of the reaction temperature on the products yields was as follows. For Pd/NaY(500/350) increasing the temperature by 23°C increases the overall CO conversion by 18%. The higher hydrocarbon yield is actually *greater* by 33% at 265°C, while at 288°C the yield of CH_4 is 140% higher than at the lower temperature. With respect to the higher hydrocarbons selectivity, the (C_2 + C_3) carbon fraction increases from 14 to 23% at the higher temperature. The fractions of olefins and linear products within each product fraction also appear to in-

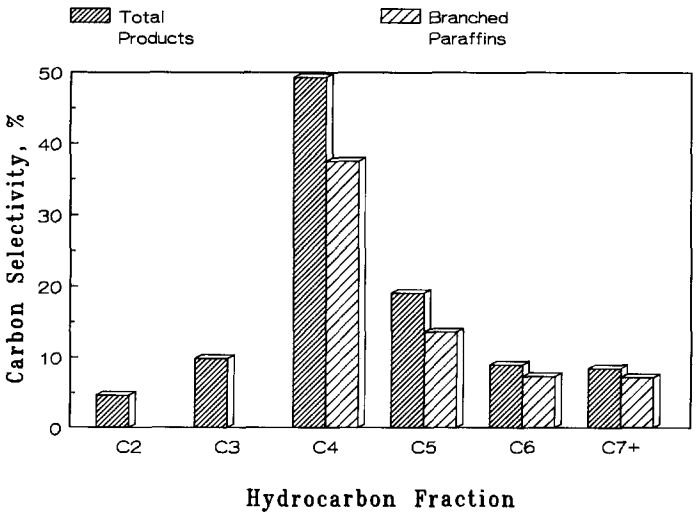

FIGURE 3

crease, but only slightly. In the case of Pd/NaY(250/250), increasing the reaction temperature from 269 to 285°C increases the overall CO conversion by 40%. However, while CH_3OH and CH_3OCH_3 yields increase by 49 and 13%, respectively, the yield of CH_4 increases by 127%.

The following procedure was used to study the effect of the space velocity on the reaction: After the catalyst had been on-stream for 20 or 24 h at a GHSV of 1800 ± 100 h^{-1} the flow rate of the reactants was reduced to give a GHSV of 900 ± 50 h^{-1}. This condition was maintained for 2 h. After this period, the flow of reactants was reduced again, giving a GHSV of 400 ± 25 h^{-1}. For Pd/NaY(500/350) the total decrease in the GHSV from 1800 to 400 h^{-1} leads to the following results:

(i) The CO conversion increases between 2.5 and 3.0 times.

(ii) The carbon selectivity toward CH_4 increases by about 30%, mostly at the expense of the higher hydrocarbons.

(iii) The (C_2 + C_3) fraction in the higher hydrocarbons increases about 20%; traces of BTX appear in the products.

(iv) Within each higher hydrocarbon product fraction, the selectivity to olefins decreases, while the selectivity toward branched paraffins remains unchanged.

For Pd/NaY(250/250) the same decrease in the GHSV results in a doubling to tripling of the CO conversion and in increases of at least 65% in the CH_4 carbon selectivity at the expense of CH_3OH and CH_3OCH_3. The carbon selectivity to higher hydrocarbons (mostly linear, up to C_7, (C_2 + C_3) fraction greater than 70%) is increased at the lower space velocities, but it never exceeds 6% of the total carbon output.

The effect of combining different calcination and reduction temperatures on the product selectivity was also studied. The behavior of Pd/NaY(500/350) and Pd/NaY(250/350) was found to be very similar. Higher hydrocarbons and CH_4 are the predominant products with these two catalysts. In contrast, Pd/NaY(250/250) produces mainly oxygenated products, some CH_4, and very little higher hydrocarbons.

Pd/HY. The time-on-stream behavior, as well as the higher hydrocarbon selectivity, for Pd/HY(500/350) is shown in Fig. 4. There is a sharp decrease in the rate of CH_4 formation during the first 2 h of reaction, Fig. 4A. Only traces of CH_3OH are detected during the reaction while no CH_3OCH_3 is

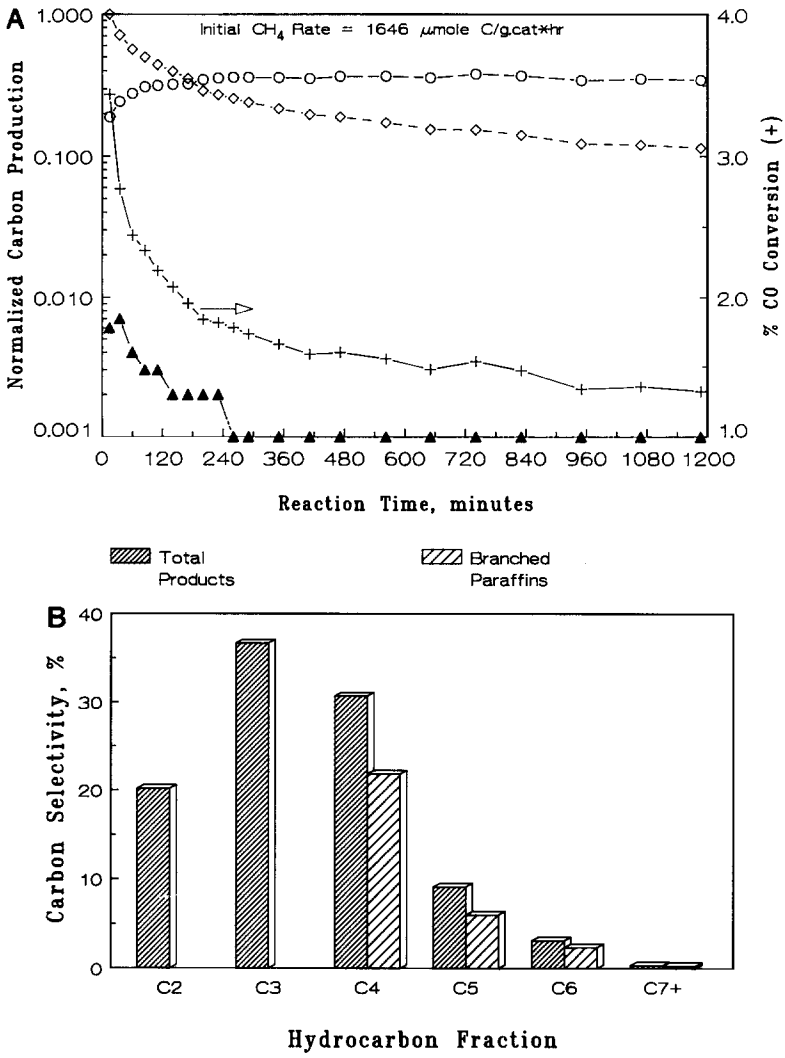

FIGURE 4

found in the products. Hydrocarbon production is high from the start of the reaction and it peaks after about 4 h on-stream when these products become the major pathway for carbon output. It slightly decreases over the next 16 h. In contrast, CH_4 formation steadily decreases and the deactivation in CO conversion during the reaction can be entirely attributed to this process. The higher hydrocarbons produced by this catalyst, Fig. 4B, consist mostly of C_2H_6, C_3H_8, and $(i + n)C_4H_{10}$, although up to C_7 hydrocarbons are detected. While lowering the GHSV from 1800 to 400 h^{-1} increases the CO conversion by 2.5 times it has no effect on CH_4 production or on the nature and size of the higher hydrocarbons formed. No olefins or BTX were detected under any of the conditions studied for this catalyst.

Mixtures of Pd/NaY and HY. The following mixtures of Pd/NaY(250/250) with HY zeolites were studied:

PMHY—A physical mixture of 0.4 g Pd/NaY(250/250) and 0.4 g of HY (the same zeolite starting material used in the preparation of Pd/HY).

TABLE 1

Higher Hydrocarbons Selectivity[a] Pattern

	$C_2 + C_3$	C_4	C_5	C_{6+}	BTX
Pd/NaY[b]	14.4	49.3	19.0	17.3	0.0
Pd/HY[b]	56.8	30.7	9.1	3.4	0.0
Pd/NaY[c] + HY (mixture)	28.5	36.0	17.3	18.2	0.0
Pd/NaY[c] + HY (series)	30.4	43.6	18.1	7.4	0.5

Note. T_R, 268 ± 3°C; P_L, 11.0 ± 0.5 atm; GHSV = 1800 ± 100 h^{-1}; $CO:H_2$ = 1:1.

[a] Carbon selectivity: (mole C in C_n fraction/mole C in C_{2+} fractions) × 100.

[b] (500/350).

[c] (250/250).

CBHY—A bed of 0.4 g of Pd/NaY(250/250) followed downstream by a 0.4 g bed of HY (the two beds were separated by one bed length of glass wool).

There is no difference between the two mixtures in the CH_4 selectivity, which is essentially due to CH_4 formation on the Pd/NaY(250/250) catalyst. However, while PMHY is highly selective toward the formation of higher hydrocarbons, CBHY produces similar amounts of higher hydrocarbons and oxygenates.

Tables 1 and 2 provide details on the nature of the higher hydrocarbons produced by these mixtures. In addition, results for Pd/NaY(500/350) and Pd/HY(500/350) are included for comparison. The data shown in these tables was obtained at nearly constant overall CO conversions (0.8 to 1.3%).

Tables 1 and 2 indicate that the two physical mixtures studied here do not behave in the same manner as the single Pd catalysts. Table 1 shows that Pd/HY is much more selective toward C_2 and C_3 formation than Pd/NaY or the HY-containing mixtures. Although our chromatographic analysis did not allow for a precise quantification of the olefinic content of the C_2 and C_3 hydrocarbons, a qualitative analysis indicates that the only case in which olefins accounted for a substantial amount (>30%) of these hydrocarbons was for CBHY. Taking into account the olefinic content of the C_4 and C_5 fractions, which were determined accu-

TABLE 2

Higher Hydrocarbons Isomer Composition

	$i-C_4:n-C_4$	% C_4H_8	$i-C_5:n-C_5$	% C_5H_{10}	$n-C_6:t-C_6$
Thermodynamic[a]	0.75		3.24		0.15
Pd/NaY[b]	3.4	1.0	2.6	1.0	0.18
Pd/HY[b]	2.5	0.0	1.9	0.0	0.2
Pd/NaY[c] + HY (mixture)	2.5	4.0	3.8	4.0	0.1
Pd/NaY[c] + HY (series)	15.7	9.0	32.3	5.0	0.0

Note. T_R, 268 ± 3°C; P_L, 11.0 ± 0.5 atm; GHSV = 1800 ± 100 h^{-1}; $CO:H_2$ = 1:1.

[a] 270°C, 1 atm.

[b] (500/350).

[c] (250/250).

rately and are shown in Table 2, the hydrogenation ability of these materials can be ranked as follows: Pd/HY > Pd/NaY > PMHY > CBHY.

It can also be seen from Table 2 that the thermodynamic equilibrium ratio $i-C_4H_{10}:n-C_4H_{10}$ is well below the values observed for the mixtures and single catalysts. However, the same is not true for the $i-C_5H_{12}:n-C_5H_{12}$ and $n-C_6H_{14}$:(total)C_6H_{14} ratios. For these hydrocarbons, a shift above the equilibrium values in the direction of the production of branched products is only observed for the mixtures, but not for the single catalysts. It is also clear from Table 2 that the HY bed alone (CBHY) converts CH_3OH and CH_3OCH_3 into branched hydrocarbons much more selectively than its physical mixture with Pd/NaY(250/250), PMHY.

There are other remarkable differences between the mixtures described here. PMHY and CBHY have entirely different deactivation behaviors with respect to higher hydrocarbons formation. In the case of PMHY the rate of higher hydrocarbon formation is still increasing even after 24 h on-stream. In contrast, for CBHY the maximum rate of higher hydrocarbons formation is observed after 4 h on-stream and during the next 20 h this rate decreases by about 25%. This decrease occurs simultaneously with an increase in the amount of unreacted CH_3OH and CH_3OCH_3 breaking through the HY bed.

Catalyst Characterization

X-Ray Diffraction

Powder diffraction patterns for NaY and Pd/NaY catalysts before and after reaction are shown in Fig. 5. These patterns clearly indicate that chemical and physical changes in the nature of Pd particles probed by this technique take place during CO hydrogenation. For Pd/NaY(250/250) and (500/350) diffraction peaks centered at $2\Theta = 40°$ (strong) and $2\Theta = 46.5°$ (broad) appear after reduction. After reaction both catalysts show new diffraction peaks centered at $2\Theta = 39°$ (strong) and at $2\Theta = 45.3°$ (weak). In the case of Pd/NaY(250/250) these peaks are the only features observed after reaction, while for Pd/NaY(500/350) some of the original peaks observed after reduction are still present.

Figure 6 shows the patterns for HY and Pd/HY catalysts. Again, extraordinary changes in the diffraction patterns of these catalysts are indicated. After reduction, sharp diffraction peaks at $2\Theta = 40°$ (strong) and $2\Theta = 46.5°$ (weaker) are present. In the case of Pd/HY(500/350) these features are almost entirely absent after reaction and a weak broad peak centered at $2\Theta = 39°$ can be seen. This feature, as well as a peak at $2\Theta = 45.3°$, are better discerned for Pd/HY (500/500) after reaction, in which case some of the original peaks observed after reduction are still present.

XPS

An analysis of the XPS characterization of Pd/NaY and Pd/HY catalysts before and after reaction as well as for bulk Pd metal indicates the following differences:

i. Shifts in the binding energy with respect to bulk Pd for the Pd $3d_{5/2}$ line are observed in the case of Pd/NaY(250/250) catalysts before and after reaction (+0.5 eV and +0.3 eV, respectively) and also for Pd/HY(500/350) (+0.3 eV before and after reaction).

ii. There is a shift of +0.5 eV in the Auger Parameter of the Pd/NaY(500/350) catalyst after reaction with respect both to the catalyst before reaction and to bulk Pd metal.

iii. Nitrogen is only detected in Pd/NaY(250/250), i.e., the catalyst that was calcined at a low temperature, so that some of the NH_3 ligands of the Pd^{2+} survived. The N : Si atomic ratio in the catalyst does not change significantly during catalysis, but a shift of +0.5 eV in the binding energy of the N 1*s* line is detected.

iv. No carbon buildup was observed for these catalysts after reaction. Only in Pd/NaY(250/250) a new carbon line appeared

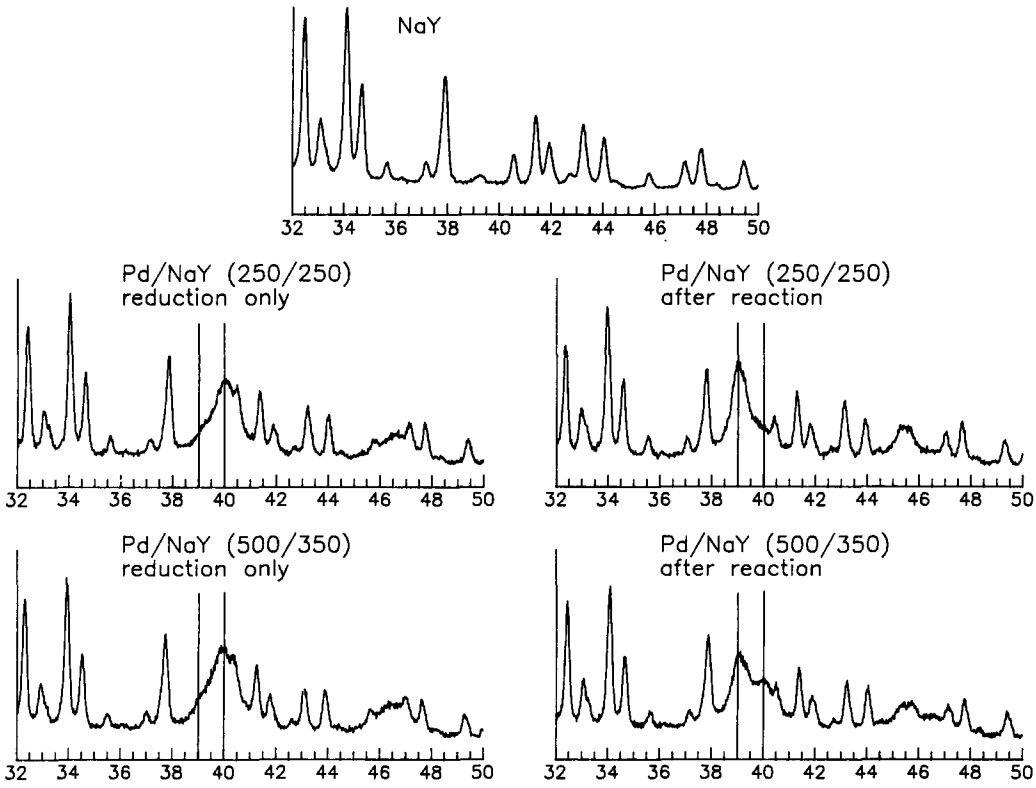

FIGURE 5

after reaction; it is shifted by +1.5 eV from the position of the background carbon line.

Figure 7 shows the Pd : Si ratios for these catalysts before and after reaction. It can be seen that while the Pd : Si atomic ratio increase significantly for Pd/NaY(250/250) and Pd/HY(500/350) after reaction, it actually decreases in the case of Pd/NaY(500/350).

DISCUSSION

Structural Changes and Catalytic Behavior

Chemical modification. The remarkable changes in the product yields during the first few hours of CO hydrogenation over Pd/NaY catalysts, as shown in Fig. 1, require comments. First, a trivial effect must be mentioned, viz. that the zeolite might act as a chromatographic column, trapping some products more until it becomes saturated with them. Although such an effect might take place during the initial stages of the reaction, a number of observations argue against it as being the main cause of the observed changes, in particular the strong dependence of initial product yields on changes in the metal dispersion in Pd/NaY. This observation has been reported previously (*11*) and is confirmed by the present data. Also restarting the reaction, after subjecting a "stable" Pd/NaY(500/350) catalyst to a 20-h reduction treatment, shows the absence of a selective holdup of products (see Fig. 2). During this reduction the zeolite pores should have been depleted of any residual reaction products. The same figure shows that only the rate of CH_4 formation is selectively enhanced, whereas formation of higher hydrocarbons and CH_3OH are only slightly affected. The formation of CH_4 throughout the reduction shows that the

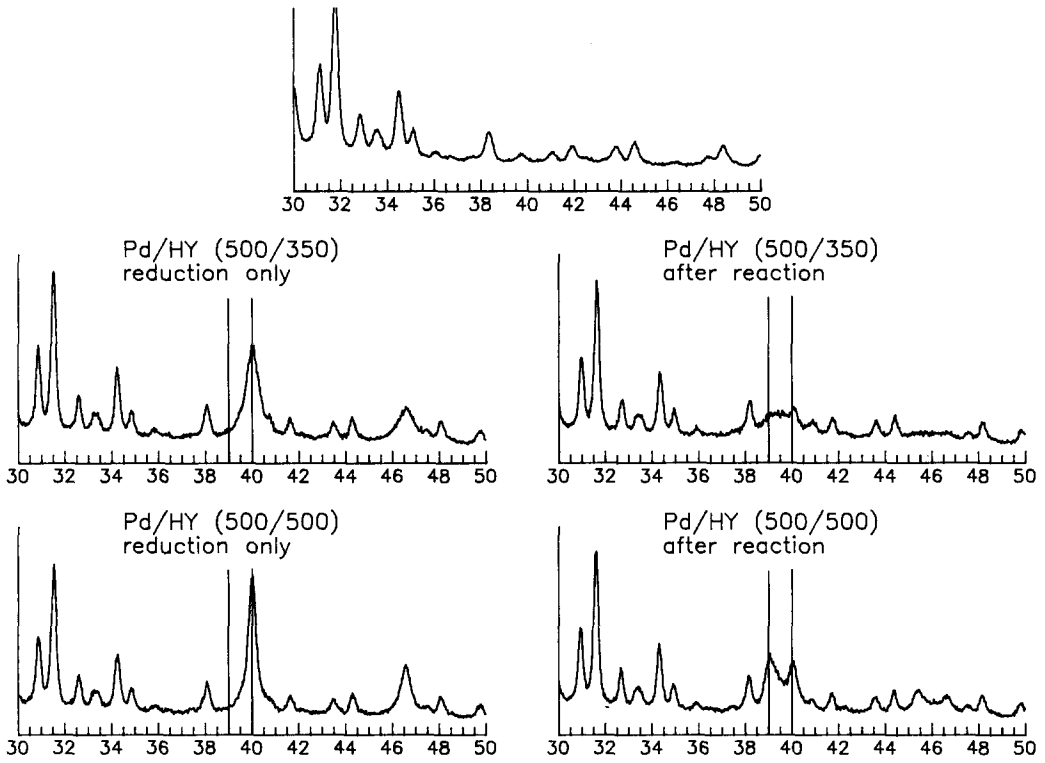

FIGURE 6

main effect of the reduction treatment is chemical removal of carbon from the Pd particles. The fast deactivation of CH_4 formation after the restart of CO hydrogenation confirms the inhibiting role of this surface carbon.

Additional evidence against the chromatographic holdup of higher hydrocarbons is provided by those catalysts (see Fig. 4A) that produce such hydrocarbons at high rates from the start of the reaction. In the case of Pd/HY(500/350) the initial rate of

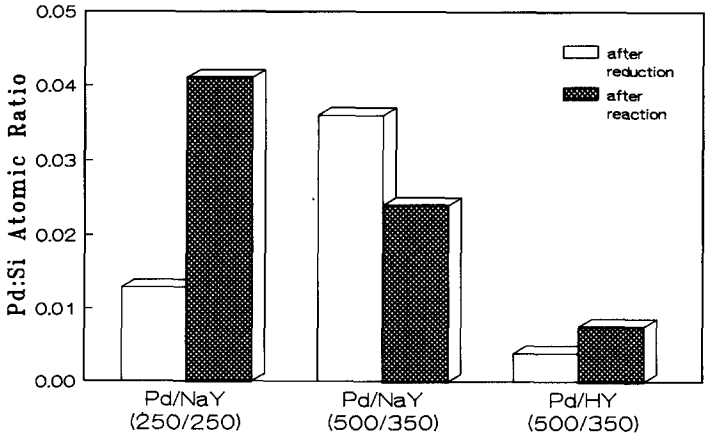

FIGURE 7

higher hydrocarbon formation is not only comparable to that of CH_4 but also significantly higher than that for Pd/NaY catalysts. Major changes in product selectivity have also been observed by other workers in the case of Pd supported on nonzeolitic materials (*24*).

The conclusion that the changes on product selectivity with time-on-stream are due to structural and chemical changes in the catalyst is supported by the XRD and XPS results.

In analyzing these data one should bear in mind that XRD only probes particles greater than approximately 30 Å. The data in Figs. 5 and 6 show that some loss of crystallinity in the zeolite framework is detectable, but this effect is small. Of much greater significance is the change in the structure of the Pd particles. Before reaction, in the reduced catalysts the peak observed at $2\Theta = 40°$ can be assigned to the Pd(111) diffraction. After reaction, a new line at $2\Theta = 39°$ is observed for several of the catalysts studied. A similar feature has been observed by Fajula *et al.* (*14*) after CO hydrogenation over Pd/NaY, Pd/HY, and Pd/SiO_2 catalysts. These authors tentatively attributed this feature to the formation of the β phase of Pd hydride. This can be safely ruled out for the present work; the only Pd hydride stable under our reaction conditions (270°C, 5 atm H_2) is the α phase (*25*), which has a lattice parameter only slightly larger than that of pure Pd. Moreover, this hydride would be destroyed when the catalysts are brought to room temperature under a He flow over a period of at least 30 min. Also any β-Pd hydride will be decomposed during such purge as was shown independently (*26*).

The large expansion of the Pd lattice observed after reaction can, however, be explained by the formation of an interstitial Pd–C compound. Although it is known that Pd does not form stable stoichiometric carbides, there are now several reports on the formation of stable supersaturated solutions of carbon in palladium having compositions of up to $PdC_{0.13}$. These phases have been identified by X-ray (*27*) and neutron (*28*) diffraction after Pd/SiO_2 and Pd black were used in C_2H_2 or C_2H_4 hydrogenation, and after exposure to CO at $T > 500°C$. Both studies also showed that the $PdC_{0.13}$ solution has a_0, the cubic unit cell parameter, of 3.99 Å (corresponding to $2\Theta = 39.07°$ for (111)) in contrast to Pd, $a_0 = 3.89$ Å (corresponding to $2\Theta = 40.12°$ for (111)). Figures 5 and 6 show that after reaction the line at $2\Theta = 40°$ is much weaker than before the reaction; a strong line near $2\Theta = 39.07°$ has emerged, indicating formation of $PdC_{0.13}$.

The measured Auger Parameter for Pd after reaction is, for all samples, equal to or slightly higher than that for the bulk metal. This shift is most pronounced for Pd/NaY(500/350), +0.5 eV, which might be tentatively ascribed to the formation of $PdC_{0.13}$. Unfortunately, there are no data in the literature to compare this tentative assignment. The observation that XPS does not show large carbon buildup is not contradictory to the proposed formation of $PdC_{0.13}$ or to the observed carbon removal during reduction after reaction since the background signal for this element is much larger than that expected from these carbon sources.

$PdC_{0.13}$ was found to have no tendency to form the β-hydride phase when exposed to H_2 and to be stable up to 600°C in an inert atmosphere and to ca. 150°C in H_2 or O_2. We have confirmed these stability limits in the following manner. The reacted Pd/NaY(500/350) catalyst used to obtain the XRD pattern in Fig. 5 was reduced at 150°C for 30 min. This resulted in no change in the position of the $PdC_{0.13}$ (111) line. However, when the same catalyst was reduced at 250°C for 16 h the $PdC_{0.13}$ (111) line disappeared entirely while the Pd (111) line appeared again at $2\Theta = 40°$.

The presence of $PdC_{0.13}$ at the end of the reaction raises a number of interesting questions. The likely source for this carbon is CO dissociation, which is also necessary for CH_4 formation. We found that even after only 1.5 h reaction most of the Pd in the

particles probed by XRD is in the form of $PdC_{0.13}$. This is also the period in which the rate of CH_4 formation decreases drastically as seen in Figs. 1 and 4A. The observation that reduction of the catalyst after reaction greatly enhances CH_4 formation with respect to other products, Fig. 2, also supports the idea that CH_4 and $PdC_{0.13}$ formation are inversely related. An alternative hypothesis, that higher hydrocarbons are a major source of C atoms in $PdC_{0.13}$ can be ruled out on the basis of two observations: First, most of the $PdC_{0.13}$ is formed in the first hour of reaction, when higher hydrocarbon formation is relatively minor. Second, $PdC_{0.13}$ is also formed in the case of Pd/NaY(250/250), as seen in Fig. 5, which produces very little higher hydrocarbons throughout the reaction, Fig. 1B.

As formation of $PdC_{0.13}$ takes place at the same stage where the rate of CH_3OH production increases, one might speculate on the role of $PdC_{0.13}$ in CH_3OH synthesis. However, the observation that production of CH_3OH (and its secondary products, CH_3OCH_3 and higher hydrocarbons) over Pd/NaY(500/350) is little affected by the destruction of $PdC_{0.13}$ during a second reduction treatment is a strong argument against this hypothesis.

Therefore, we propose the following explanation for the formation of $PdC_{0.13}$. When small Pd particles, which expose highly unsaturated Pd atoms, are initially exposed to CO this reactant is dissociatively chemisorbed leading to elemental carbon formation. Part of this carbon is hydrogenated to CH_4 and part is incorporated into the Pd particles to form $PdC_{0.13}$. The formation of this solution results in less CH_4 formation, possibly by changing the propensity of the Pd particles for hydrogen chemisorption, parallel to the total inability of $PdC_{0.13}$ to *ab*sorb hydrogen. The suppression of hydrogen solubility of $PdC_{0.13}$ as compared to pure Pd has been discussed by Boudart and Hwang (*26*) in terms of kinetic,thermodynamic, steric, and electronic reasons. If decreasing CH_4 production is indicative of increasing formation of $PdC_{0.13}$, it follows that it is rapidly formed at the start of the reaction but continues for an extended period of time.

Particle size changes. So far we have discussed changes in the product distribution during reaction in terms of the formation of $PdC_{0.13}$. However, this does not appear to be the only process involved. The XPS results provide evidence that processes involving particle growth, redispersion, migration, and restructuring also take place in the initial stages of the reaction. In particular, the significant differences in the Pd : Si ratios measured before and after reaction might be the result of particle migration or growth or a combination of both. Presently we are unable to deconvolute these processes and can only conclude that dynamic changes involving the Pd particles do take place with reaction and that there is no evidence for a preferential accumulation of Pd in the outer region of the zeolite crystallites with respect to its interior. We have recently obtained further evidence for the latter assertion using TEM. This technique showed that although there are some very large particles (>1000 Å) on the outer surface after reaction, most of the Pd is present in particles (having diameters in the 30 to 60 Å range), which remain entrapped inside the zeolite channels.

For most catalysts studied here the Pd $3d_{5/2}$ binding energy is close to that of the bulk metal. In accordance with the XRD data this can be attributed to the formation of relatively large (>30 Å) Pd or $PdC_{0.13}$ particles. However, for Pd/NaY(250/250) and Pd/HY(500/350) shifts of 0.3–0.5 eV were found. This might be attributed to the presence of a significant fraction of small particles since the position of the Pd $3d_{5/2}$ line is determined by the relative fraction of large and small particles in the near surface region of the zeolite crystallites. For Pd/HY(500/350), the larger fraction of small particles might be due to their stabilization by the

high concentration of protons, while for Pd/NaY(250/250) the milder reduction condition may play a role.

The catalytic behavior of Pd/HY(500/350) shows similarities to that of Pd/NaY(500/350). There is a sharp decrease in the initial rate of CH_4 formation (Fig. 4A). Drastic changes in the XRD pattern are also observed (Fig. 6), the appearance of $PdC_{0.13}$ being clearly visible in the case of Pd/HY(500/500). It should be noted that the XRD pattern for Pd/HY(500/350) indicates the disappearance of large particles from the catalyst after reaction. We have also observed a similar phenomenon in the case of Pd–Ni/NaY catalysts used in CO hydrogenation (*29*).

As discussed above, the transformations in the Pd/NaY catalysts that are responsible for the large change in the initial rate of formation of CH_3OH (and its secondary products) seem to be irreversible, at least with respect to a second reduction of the catalyst after its use. We suggested previously that this was in part due to a process of particle growth (*13*). We have now confirmed using EXAFS that exposure of small Pd clusters in Pd/NaY to CO at 1 atmosphere and temperatures as low as 50°C results in the irreversible growth of the Pd particles (*30*). It seems reasonable to extrapolate that under our reaction conditions such phenomenon is also possible. CO-induced restructuring of Pd particles (*20–22*) has now been documented by other groups as well. Several studies have shown that CO dissociation increases with Pd dispersion (*21, 22, 31, 32*) and that the CO heat of chemisorption appears to increase sharply as the Pd crystallite size decreases below 30 Å (*33*). CH_3OH decomposition to CO and H_2 on Pd/Al_2O_3 catalysts has also been found to increase with Pd dispersion, although the situation was found to be more complex for Pd/TiO_2 and Pd/ZrO_2 catalysts (*34*).

The totality of this evidence suggests that both CH_4 and CH_3OH formation are strongly structure-sensitive reactions. At the start of the reaction small Pd particles, which occupy the supercages, are present. These particles dissociate CO easily and form CH_4. This process also initiates $PdC_{0.13}$ formation. At the same time, CO-induced particle growth takes place. It is this Pd particle growth that leads to local destruction of the zeolite framework causing distinct changes in the XRD patterns (see Figs. 5 and 6) before and after reaction. Electron microscopy shows that Pd particles larger than supercages are formed. On these larger $PdC_{0.13}$ particles, CH_4 formation is suppressed and CH_3OH production is favored. Due to the strong changes of the Pd particle morphology during reaction conditions it does not appear meaningful to express measured rates as turnover frequencies.

Higher Hydrocarbons Formation and Reaction Mechanism

Up to this point we have considered only the formation of CH_4 and CH_3OH, which takes place exclusively on the Pd particles. The formation of CH_3OCH_3 and higher hydrocarbons requires acid sites, albeit of a different nature. The conversion of CH_3OH to CH_3OCH_3 is known to take place easily even over weakly acidic supports. However, conversion of CH_3OH and CH_3OCH_3 to higher hydrocarbons requires stronger Brønsted acid sites. The different acid strength requirements for these reactions is illustrated by the product selectivity of the Pd/NaY catalysts. For Pd/NaY(500/350), two Brønsted acid sites are formed during the reduction of each Pd^{2+} ion present after calcination at 500°C. This leads to the formation of higher hydrocarbons as illustrated in Figs. 1A and 3. However, when Pd/NaY catalysts are calcined to 250°C only, $[Pd(NH_3)_2]^{2+}$ rather than Pd^{2+} ions are formed. During the reduction of this complex, NH_3, which reacts with H^+ formed during this process to give NH_4^+ ions, is liberated. This "neutralized" Pd/NaY(250/250) catalyst is incapable of forming higher hydrocarbons since it lacks Brønsted acid sites, but it is still able to convert CH_3OH

to CH_3OCH_3 as seen in Fig. 1B. The XPS results indicate that the NH_4^+ ions formed in this catalyst react during CO hydrogenation to give new nitrogen-containing ions, which seem to be stable up to about 300°C. However, if calcination at 250°C is followed by reduction at 350°C, NH_4^+ ions are no longer stable; their decomposition results in the formation of protons. This Pd/NaY(250/350) catalyst then behaves exactly the same as the Pd/NaY(500/350) catalyst.

Higher reaction temperatures favor CH_4 production. This is surprising since CH_4 formation from CO and H_2 is twice as exothermic as CH_3OH formation. Therefore, the reason for this behavior must be kinetically related. Since CH_4 formation requires CO dissociation and Pd is a metal on which this process is not easily carried out, the logical explanation for this temperature dependence is that higher temperatures favor the dissociative chemisorption of CO. Room-temperature nondissociative and high-temperature dissociative CO chemisorption on Pd have been reported in several studies (*21, 22, 31*). The observation that the yield of higher hydrocarbons is actually greater at 265°C than at 288°C for Pd/NaY(500/350) and that CH_3OH and CH_3OCH_3 yields decrease considerably less than that of CH_4 when the reaction temperature is lowered for Pd/NaY(250/250) can also be explained in terms of the competitive rates of CO dissociative and nondissociative chemisorption. This indicates that CH_4 and CH_3OH are formed by two entirely distinct pathways, which have different CO chemisorption strength requirements.

Although Pd/NaY(500/350) and Pd/HY(500/350) produce higher hydrocarbons selectively, a comparison of Figs. 3 and 4B and of Tables 1 and 2 shows that the nature of these hydrocarbons is considerably different. For example, (C_2 + C_3) hydrocarbons contain approximately 15% of the carbon present in higher hydrocarbons in the case of Pd/NaY(500/350) versus 57% for Pd/HY(500/350). Overall, chain growth is greatly inhibited for Pd/HY(500/350) compared to Pd/NaY(500/350). In addition, the higher hydrocarbons formed over Pd/HY(500/350) are less branched than for Pd/NaY(500/350), and no olefin formation is observed over the former while there is a small but significant olefin production over the latter.

To understand these differences in the higher hydrocarbon selectivity it is useful to turn to the results obtained with different physical mixtures (Tables 1 and 2). It is clear that higher hydrocarbons formation on pure HY, as seen for CBHY, is characterized by the selective formation of hydrocarbons having four or more carbon atoms that are almost exclusively branched, by the presence of olefins (in particular in the C_2 and C_3 fractions), by the presence of a small fraction of BTX products and by a relatively high deactivation rate of the acid function. Bringing the acid sites in HY in closer proximity to the Pd particles, as in the case of PMHY, results in an increase in the formation of higher hydrocarbons (in particular having six or more carbon atoms), in a large decrease in the formation of branched products and in the suppression of olefin and BTX formation as well as less acid function deactivation. These trends are continued in the case of Pd/NaY(500/350), in which H^+ and Pd particles coexist within a very short distance. However, keeping the H^+–Pd particle distance relatively constant but increasing the concentration of the former, as in Pd/HY(500/350), completely changes the nature of the higher hydrocarbons formed.

We believe that these selectivity patterns can be rationalized in the following manner: CH_3OH and CH_3OCH_3 conversion on Brønsted acid sites leads to the higher hydrocarbon distribution characteristic of CBHY. The presence of Pd particles in proximity to these acid sites opens up the possibility for the readsorption of hydrocarbons on the Pd particles. Olefins can then be hydrogenated. Hydrocarbon products desorbing from the Pd particles can also be readsorbed on acid sites and react further.

These phemonema can already be seen in

the case of PMHY, where intercrystallite diffusion of products is possible. Readsorption and hydrogenation of hydrocarbons on the Pd particles results in a decrease in the iso : normal ratio of the C_{4+} products, in an increase in the C_{6+} hydrocarbon selectivity, and in a decrease in the olefinic fraction of the products, which is probably the cause for the suppression in BTX formation and acid function deactivation. The close proximity of H^+ and Pd particles in Pd/NaY(500/350) enhances the transport of products between these sites. This results in a large increase in the fraction of C_{4+}, products at the expense of (C_2 + C_3) hydrocarbons and in a further decrease in the iso : normal ratios. Hydrogenation of olefinic products is also enhanced over this catalyst.

The product selectivity of Pd/HY(500/350) can be understood in terms of a greatly enhanced hydrogenation ability of the Pd particles. This is reflected in the total lack of olefins in the products as well as the much enhanced selectivity toward (C_2 + C_3) hydrocarbons, which is actually higher than for pure HY. It has been shown previously that the benzene hydrogenation ability of Pd/Y catalysts followed the order Pd/HY ≫ Pd/NaY (*35*). We assume that C_2 and C_3 olefins, which have been proposed to be the initial products and chain initiators for hydrocarbon growth during CH_3OH and CH_3OCH_3 conversion on the acid sites of HZSM-5 (*36*), are readsorbed on Pd particles and efficiently hydrogenated preventing further chain growth. An alternative hypothesis would assume that higher hydrocarbons are hydrogenolyzed (on Pd particles or protons) producing an excess (C_2 + C_3) hydrocarbons. This seems, however, less likely since these reactions are known to be slow under the present conditions.

It is obvious that the presence of Pd leads to a much lower olefin/paraffin ratio than in the MTG process; obviously the hydrogenation activity of Pd is not suppressed by the presence of CO. A much more surprising observation is that the presence of Pd particles in proximity to the acid sites results in a drastic lowering in the selectivity toward branched products. We have no conclusive explanation for this. It might be related to an observation reported by Tau *et al.* (*37*) that the reaction of propane with a methanol-derived C_1 species differs significantly from that of the C_3 species that is involved in the production of C_4 and higher hydrocarbons in the normal MTG reaction pathway over HZSM-5.

CONCLUSIONS

There is strong evidence that remarkable chemical and physical changes in the nature of the Pd particles take place during reaction. The former include the formation of a $PdC_{0.13}$ solution, which was confirmed by XRD and chemical methods. XPS analysis also indicates chemical and physical changes in various aspects of the catalysts, in particular with respect to Pd particle growth, redispersion, and migration. The nature of the CO hydrogenation reaction is likewise complicated. It involves structure sensitivity in CH_4 and CH_3OH formation, the reaction of CH_3OH to form CH_3OCH_3 over weak acid sites, and the conversion of both products to hydrocarbons over Brønsted acid sites. Readsorption of hydrocarbons on Pd particles and their subsequent hydrogenation affect the activity, selectivity, and deactivation of the catalysts.

ACKNOWLEDGMENTS

Financial support of the National Science Foundation, Contract CTS-8911184, and a grant-in-aid by the Engelhard Corporation are gratefully acknowledged.

REFERENCES

1. Pichler, H., *in* "Advances in Catalysis" (W. G. Frankenburg, V. I. Komarewsky, and E. K. Rideal, Eds.), Vol. 4, p. 271. Academic Press, New York, 1952.
2. Chang, C. D., "Hydrocarbons from Methanol." Dekker, New York, 1983.
3. Poutsma, M. L., Elek, L. F., Ibarbia, P. A., Risch, A. P., and Rabo, J. A., *J. Catal.* **52,** 157 (1979).
4. Berlowitz, P. J., and Goodman, D. W., *J. Catal.* **108,** 364 (1987).
5. Nonneman, L. E. Y., and Ponec, V., *Catal. Lett.* **7,** 197 (1990).

6. Caesar, P. D., Brennan, J. A., Garwood, W. E., and Ciric, J., *J. Catal.* **56,** 274 (1979).
7. Chang, C. D., Lang, W. H., and Silvestri, A. J., *J. Catal.* **56,** 268 (1979).
8. Fujimoto, K., Kudo, Y., and Tominaga, H., *J. Catal.* **87,** 136 (1984).
9. Saha, N. C., and Wolf, E. E., *Appl. Catal.* **13,** 101 (1984).
10. Kikuzono, Y., Kagami, S., Naito, S., Onishi, T., and Tamaru, K., *Faraday Discuss. Chem. Soc.* **72,** 135 (1981).
11. Thomson, R. T., and Wolf, E. E., *Appl. Catal.* **41,** 65 (1988).
12. Thomson, R., Montes, C., Davis, M. E., and Wolf, E. E., *J. Catal.* **124,** 401 (1990).
13. Cavalcanti, F. A. P., Dossi, C., Sheu, L. L., and Sachtler, W. M. H., *Catal. Lett.* **6,** 289 (1990).
14. Fajula, F., Anthony, R. G., and Lunsford, J. H., *J. Catal.* **73,** 237 (1982).
15. Choudary, B. M., Matusek, K., Bogyay, I., and Guczi, L., *J. Catal.* **122,** 320 (1990).
16. a. Homeyer, S. T., and Sachtler, W. M. H., *J. Catal.* **117,** 91 (1989); b. **118,** 266 (1989).
17. a. Sheu, L. L., Knözinger, H., and Sachtler, W. M. H., *Catal. Lett.* **2,** 129 (1989); b. Sheu, L. L., Knözinger, H., and Sachtler, W. M. H., *J. Am. Chem. Soc.* **111,** 8125 (1989).
18. Zhang, Z., Chen, H., Sheu, L. L., and Sachtler, W. M. H., *J. Catal.*, **127,** 213 (1991).
19. Raval, R., Haq, S., Harrison, M. A., Blyholder, G., and King, D. A., *Chem. Phys. Lett.* **167,** 391 (1990).
20. Hicks, R. F., Qi, H., Kooh, A. B., and Fischel, L. B., *J. Catal.* **124,** 488 (1990).
21. Gillet, E., Channakhone, S., Matolin, V., and Gillet, M., *Surf. Sci.* **152/153,** 603 (1985).
22. Matolin, V., Gillet, E., Reed, N. M., and Vickerman, J. C., *J. Chem. Soc. Faraday Trans. 1* **86,** 2749 (1990).
23. Wagner, C. D., *Faraday Discuss. Chem. Soc.* **60,** 291 (1975).
24. Driessen, J. M., Poels, E. K., Hindermann, J. P., and Ponec, V., *J. Catal.* **82,** 26 (1983).
25. Brodowsky, H., and Wicke, E, *in* "Topics in Applied Physics" (G. Alefeld and J. Völkl, Eds.), Vol. 29, p. 73. Springer-Verlag, Berlin, 1978.
26. Boudart, M., and Hwang, H. S., *J. Catal.* **39,** 44 (1975).
27. Stachurski, J., *J. Chem. Soc. Faraday Trans. 1* **81,** 2813 (1985).
28. Ziemecki, S. B., Jones, G. A., Swartzfager, D. G., Harlow, R. L., and Faber, J., Jr., *J. Am. Chem. Soc.* **107,** 4547 (1985).
29. Feeley, J., Cavalcanti, F. A. P., Stakheev, A.Yu., and Sachtler, W. M. H., *J. Catal.*, submitted.
30. Unpublished results.
31. Kruse, N., and Gillet, E., *Z. Phys. D: Atoms Mol. Clusters* **12,** 575 (1989).
32. Ichikawa, S., Poppa, H., and Boudart, M., *J. Catal.* **91,** 1 (1985).
33. Chou, P., and Vannice, M. A., *J. Catal.* **104,** 17 (1987).
34. Saitoh, Y., Ohtsu, S., Makie, Y., Okada, T., Satoh, K., Tsuruta, N., and Terunuma, Y., *Bull. Chem. Soc. Jpn.* **63,** 108 (1990).
35. Figueras, F., Gomez, R., and Primet, M., *Adv. Chem. Ser.*, **121,** 480 (1973).
36. Mobile work.
37. Tau, L.-M., Bao, S.-Q., and Davis, B. H., *J. Catal.* **114,** 190 (1988).